Technical Paper

ISSN 1996-6814 Int. J. Pavement Res. Technol. 6(4):287-293

Evaluating Wet Weather Driving Benefits Of Grooved Pavements

Fenghua Ju[1], Tien Fang Fwa[1], and Ghim Ping Ong[1+]

Abstract: Under wet conditions, vehicles running on wet roads may experience low skid resistance and hydroplaning. Past research has shown that grooving of pavement reduces the risk of hydroplaning and increases tire-pavement skid resistance. A number of locked-wheel skid resistance models are available for hydroplaning speed and skid resistance evaluation and prediction. However, today, most automobiles are equipped with antilock braking systems (ABS) to prevent wheel locking. This paper presents an evaluation of wet weather driving benefits of pavement grooving utilizing an improved skid resistance simulation model for automobiles with ABS. The mechanism by which pavement grooving improves the skid resistance of pavements for both locked and rolling wheels are examined. Based on an analytical study, it is found that the use of ABS with pavement grooving improves wet pavement skid resistance values by 54% to 366% and reduces braking distances by 26.9% to 71.8% as compared to locked wheels braking on smooth pavement surface under various operational condition.

DOI:10.6135/ijprt.org.tw/2013.6(4).287
***Key words**: Antilock braking system; Braking distance; Pavement grooves; Skid resistance.*

Introduction

Pavement skid resistance during wet weather is substantially reduced from its dry-weather value. This reduced skid resistance level can lead to a longer braking distance and increase the risk of hydroplaning occurrence [1, 2]. It is known that grooving of pavement can drain water trapped at tire-pavement interface through the groove channels, therefore increase pavement skid resistance. Past studies have shown that pavement grooving is a good technique to maintain adequate macrotexture and skid resistance on pavement surface [3-5]. However, no insight has been given into the mechanism by which pavement grooving improves the skid resistance of pavement surfaces.

Nowadays most vehicles are equipped with antilock braking system (ABS) for safety purpose. By controlling wheel slip during braking, wheel locking is prevented and the available braking force is kept at or close to the maximum. The use of ABS was known to improve skid resistance and braking performance [6]. Much past studies have been performed for improvising ABS controls to provide better vehicle braking and directional control [7-9], but little effort has been made in modeling the effects of ABS on skid resistance in a mechanistic manner.

The objective of this paper is to evaluate the wet weather driving benefits of grooved pavements to provide an insight into the mechanism by which pavement grooving improves the skid resistance of pavement surfaces for unlocked wheel. The development of an improved simulation model for the interaction between a wetted pavement and an automobile tire with ABS is presented in this paper.

[1] Department of Civil & Environmental Engineering, National University of Singapore, Block E1A, 1 Engineering Drive 2, # 07-03, Singapore 117576.
[+] Corresponding Author: E-mail ceeongr@nus.edu.sg
Note: Submitted January 15, 2013; Revised June 23, 2013; Accepted June 23, 2013.

Finite Element Skid Resistance Simulation Model Considering ABS Control

Concept of Tire Slip and Use of Antilock Braking System

When the brake is applied to an automobile travelling on the road, a braking force will be generated to impede vehicle motion [10]. Before the wheel is fully locked, there is a difference existing between the velocity of the slipping tire tread and the translation speed of the vehicle. This difference is defined as tire slip ratio and is calculated by the following equation:

$$S = \frac{v - r\omega}{v} \tag{1}$$

where S represents the tire slip ratio, v is the translation speed of vehicle, ω is the tire angular velocity, and r is the effective tire-rolling radius. When tire slip ratio S is close to zero, it means that a vehicle is in its normal driving condition. When tire slip ratio S increases to one, it represents a locked wheel condition. Under the locked wheel condition, directional control is lost and the braking distance becomes longer.

Fig. 1 shows a typical non-linear relationship between tire slip ratio and tire longitudinal friction coefficient. It can be observed from the figure that friction coefficient increases from zero slip (i.e. driving state) to an optimum slip ratio and then decreases until the wheel is locked. The optimum slip ratio is the most desirable a driver would prefer during braking since its frictional coefficient is at a higher level as compared to that experienced in the locked wheel condition. As such, most automobiles today are equipped with an antilock braking system (ABS) to maintain a slip at or close to the optimum slip ratio. Past research studies have shown that the optimum slip ratio lies between 0.10 and 0.20 [10-12]. Most antilock braking systems attempt to keep the slip within this optimal slip range of 0.10 to 0.20 and avoid the situation where the wheels get locked. Therefore, an optimum slip ratio is assumed as 0.15 in this paper.

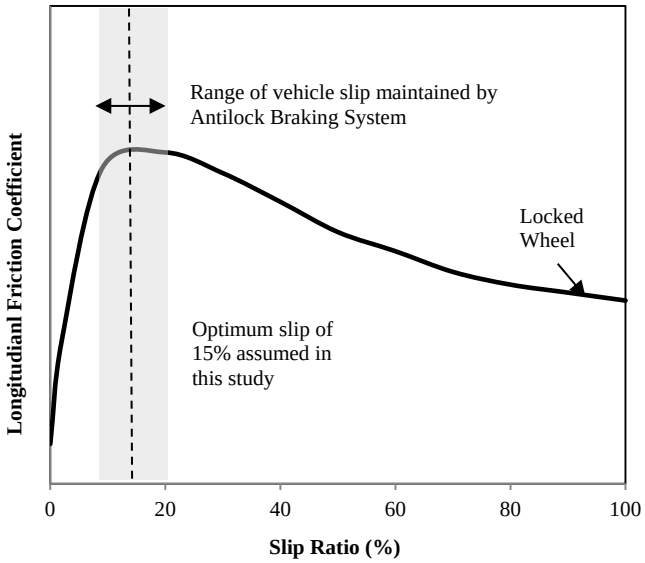

Fig. 1. Relationship between Tire Slip Ratio and Longitudinal Friction Coefficient.

Simulation Model of Skid Resistance Considering Vehicle Slip

This paper assumes that the wheel travels along a straight line with a given speed and slip ratio. Fig. 2 depicts the three-dimensional finite element model developed in this paper using the finite element computer code ADINA [13, 14]. This simulation model has been modified from one developed by Ong and Fwa [15, 16] to model the effect of ABS. Basically, the model was developed considering theoretical structural mechanics and computation fluid dynamics principles. The ASTM 524 standard smooth tire [17] is adopted to study the skid resistance characteristics of the tire subjected to the effects of ABS on both smooth and grooved pavements. The tire model is developed using four-node iso-parametric single-layer shell elements. The pavement surface is assumed to be ideally rigid and is modeled using single-layer elements. The fluid sub-model is developed using four-node tetrahedral elements. For the problems studied in the paper, 8,100, 2,400 and 26,432 elements for the tire, pavement and fluid model were found to give sufficiently accurate results. The key parameters to the simulation model are listed below.

- Tire dimensions - tire radius and width for the ASTM E524 tire [17]
- Tire inflation pressure of 165.5 kPa;
- Tire rim is assumed to be rigid with an elastic modulus of 100 GPa, a Poisson's ratio of 0.3, and a density of 2700 kg/m^3;
- Tire sidewalls are of an assumed isotropic elastic material with a composite elastic modulus of 20 MPa, a Poisson's ratio of 0.45 and a density of 1200 kg/m^3;
- Tire tread rubber is assumed to be of a homogeneous, isotropic elastic material with a composite elastic modulus of 100 MPa, a Poisson's ratio of 0.45 and a density of 1200 kg/m^3;
- Wheel load of 4800 N is specified;
- Water is assumed to be incompressible and its properties at 25° C are used, i.e. density, dynamic viscosity and kinematic viscosity are 997.1 kg/m^3, 0.894×10^3 N.s/m^3 and 0.897×10^6 m^2/s respectively;
- Water film thickness on pavement surface is varied in the simulation;
- Vehicle speed and slip can be varied in the simulation;
- Pavement is modeled as a rigid layer; and
- Pavement grade is assumed to be zero

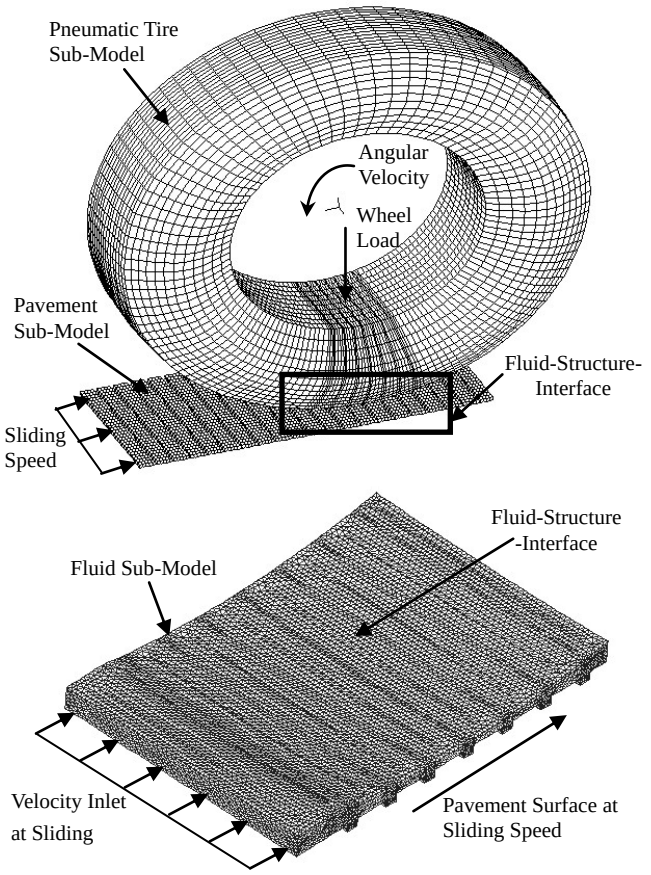

Fig. 2. Skid Resistance Simulation Model Taking into Account of Vehicle Slip.

The tire had been calibrated and validated in the authors' previous works for the standard ASTM E-274 locked wheel skid tests [18]. It was found in these studies that the simulation produces results that were sufficiently close to experimentally-collected locked wheel skid data.

Determination of Skid Resistance for Rolling Tires

The finite element model produces output data in terms of fluid drag force, and fluid uplift force due to tire-fluid interaction as tire-pavement contact reaction force. Skid resistance experienced by a rolling tire can be calculated as follow:

$$SN_{s,v} = \frac{F_x}{F_z}\times 100 \cdot \tag{2}$$

where $SN_{s,v}$ is the skid number at speed v [km/h] with slip ratio s, F_x is the horizontal resistance force to motion acting on the tire tread and F_z is the vertical wheel load. The horizontal resistance force F_x is the sum of the traction force due to tire-pavement interaction and the fluid drag force developed at the tire-fluid interface.

Pavement Surfaces Considered in Study

The driving benefits of pavement grooves on wet pavement are studied using the experimental data obtained by Horne and Tanner [19]. Two types of pavement surface are examined in this paper. They are:

- burlap drag concrete surface
- burlap drag concrete surface transversely grooved with 6.36 mm groove depth and groove width at a center-to-center spacing of 25.4 mm.

Validation of Simulation Model

Validation of the modified numerical simulation model is performed against experimental results conducted by Horne and Tanner [19]. Two water depths are used in this study. The first water film thickness is 0.5 mm. The second wetness condition is classified as flooded with 3.8 mm water-film thickness. The tire adopted in this study is ASTM 524 bald-tread tire. Both the locked wheel and braking wheel optimized by the anti-locked system are considered in the model. Tables 1 and 2 show the comparison between the results from the simulation model against the experimental SN value. It can be seen from the table that the difference in skid number is mostly within the range of ±3 SN units. This indicates the ability of this model in simulating skid resistance for rolling tires moving on wet pavements at a given slip.

Evaluating the Driving Benefits of Pavement Grooves on Wet Pavement Skid Resistance

Past research studies had noted the effectiveness of antilock braking systems in providing superior skid resistance performance [10, 11] as compared to the extreme situation where a wheel gets locked during skidding. To illustrate the driving benefits of ABS, this paper employs the developed simulation model to evaluate the effects of ABS on skid resistance for different water-film thicknesses and compare it against locked wheel skid resistance.

Table 3 shows the simulation results of the locked wheel skid numbers and the skid numbers experienced by the rolling tire at the optimum slip ratio for each pavement surface with varying water film thicknesses. Two additional water-film thicknesses, 1.0mm and 7.5 mm respectively, are also examined using the finite element simulation model to study the effects of water thickness.

Table 4 further compares the skid number experienced by the locked wheel and that by the wheel at optimum slip under different pavement surface conditions, water-film thicknesses and speeds. From this table, it can be observed that:

Table 1. Comparison between Simulation and Experimental Skid Number for Locked Tires.

Pavement Surface Type	Water Depth [mm]	Test Speed v [km/h]	Experimental SN_{locked}	Predicted SN_{locked}	Error	% Error	Back-calculated $SN_{locked,0}$
Ungrooved Pavement	0.5	32	62.5	62.3	0.2	0.4	64
		64	41.7	41.2	0.5	1.2	
		96	30	28.3	1.7	5.7	
	3.8	32	60	58.5	1.5	2.5	64
		64	24.2	28.0	-1.3	-4.7	
		96	17.5	17.8	1.5	7.8	
Grooved Pavement	0.5	32	65.8	68.1	-2.3	-3.5	70
		64	61	60.4	0.6	0.9	
		96	54.2	55.1	-0.9	-1.6	
	3.8	32	65.2	67.6	-2.4	-13.7	70
		64	60	58.9	1.1	1.8	
		96	52.5	53.8	-1.3	-2.4	

Table 2. Comparison between Simulation and Experimental Skid Number for Slipping Tires.

Pavement surface type	Water Depth [mm]	Test Speed v [km/h]	Experimental SN_{ABS}	Predicted SN_{ABS}	Error	% Error	Back-calculated $SN_{ABS,0}$
Ungrooved Pavement	0.5	32	90.8	87.1	3.7	4.1	88
		64	70.8	73.6	-2.8	-4.0	
		96	54.2	51.7	-2.5	4.5	
	3.8	32	87.6	86.1	1.5	2.5	88
		64	59.3	52.1	7.2	12.1	
		96	37.5	37.4	0.1	0.2	
Grooved Pavement	0.5	32	94.2	96.0	-1.8	-1.9	97
		64	89.2	88.4	0.8	0.9	
		96	86.7	84.6	2.1	2.4	
	3.8	32	95	95.3	0.3	0.3	97
		64	84.2	85.8	-1.6	-1.8	
		96	76.7	78.7	-2.0	-2.6	

Table 3. Skid Numbers for Different Pavements with Varying Speeds and Water-film Thicknesses.

Pavement Surface Type	Water Depth [mm]	Speed v [km/h]	$SN_{locked,v}$	$SN_{ABS,v}$
Ungrooved Pavement	1.0	32	60.8	85.7
		64	38.3	73.4
		96	24.1	48.7
	7.5	32	55.3	79.4
		64	23.8	40.8
		96	15.6	29.0
Grooved Pavement	1.0	32	68.0	95.6
		64	59.4	86.8
		96	54.7	82.5
	7.5	32	67.3	94.5
		64	57.3	80.3
		96	46.0	72.7

- the application of ABS control and transverse groove is able to provide the highest improvement of skid resistance when compared to other driving conditions.
- the skid numbers for all cases decrease as speed increases. This is in agreement with findings of past research [20, 21].

Determination of Braking Distance on Pavement

With the calculated skid number presented in last section, the effects of pavement grooving and ABS control on braking distance can be mechanistically evaluated and compared.

Methodology for Braking Distance Computation

The braking distance is computed based on the method proposed by Ong and Fwa [22]. It has been defined that braking distance D is equal to the distance travelled by the vehicle from the moment brake is applied to the moment of complete stop. This distance D can be calculated using the following equation:

$$D = \int_0^T v(t)\,dt \tag{3}$$

where $v(t)$ is the vehicle speed at time t, $t = 0$ is the time application of brake, $t = T$ is the time when vehicle comes to a complete stop, and Δx represents the distance travelled over an incremental time period Δt.

The vehicle speed at time t can be computed at:

$$v(t) = v\left(t - \frac{\Delta t}{2}\right) - \int_{t-\Delta t/2}^{t+\Delta t/2} a(t)\,dt \tag{4}$$

where $a(t)$ is the deceleration rate of the vehicle. The deceleration rate of the vehicle is a function of the pavement skid resistance and pavement grade, as shown in Eq. (3),

$$a(t) = \left[\mu(t) + G\right] g \tag{5}$$

where $\mu(t)$ is the coefficient of friction between the tire and wet pavement surface, G is the grade of the pavement and g is the acceleration due to gravity. Pavement skid resistance is numerically related to the tire-pavement coefficient of friction $\mu(t)$ by the following equation:

$$\mu = 0.01(SN) \tag{6}$$

This analysis assumes that pavement grade is equal to zero. Thus Eq. (1) can be reformulated as:

$$D = \int_0^T v(t)dt = \int_0^T \left[v\left(t - \frac{\Delta t}{2}\right) - \int_{t-\Delta t/2}^{t+\Delta t/2} 0.01SN(t)dt \right] dt \tag{7}$$

Eq. (5) provides the computational basis for evaluating braking distance.

Skid resistance are affected by tire properties, pavement surface characteristics, vehicle properties and environmental conditions, therefore the skid number SN can be further expressed as:

$$SN = f\,(v, p_t, t_w, P, SN_0, w, d, s, \Theta) \tag{8}$$

This equation indicated that skid resistance is dependent on vehicle speed (v), tire inflation pressure (p_t), water-film thickness

Table 4. Percentage Improvement in Skid Number Due to Groove and ABS Application.

Water-film Thickness [mm]	Initial Vehicle Speed [km/h]	Percentage Improvement in Skid Number Due to		
		Groove Application for Locked Wheel Case	ABS Application for Smooth Pavement	Groove and ABS Application
0.5	32	9.3%	39.8%	54.1%
0.5	64	46.6%	78.6%	114.6%
0.5	96	94.7%	82.7%	198.9%
1.0	32	11.8%	41.0%	57.2%
1.0	64	55.1%	91.6%	126.6%
1.0	96	127.0%	102.1%	242.3%
3.8	32	15.6%	47.2%	62.9%
3.8	64	110.4%	86.1%	206.4%
3.8	96	202.2%	110.1%	342.1%
7.5	32	21.7%	43.6%	70.9%
7.5	64	140.8%	71.4%	237.4%
7.5	96	194.9%	85.9%	366.0%

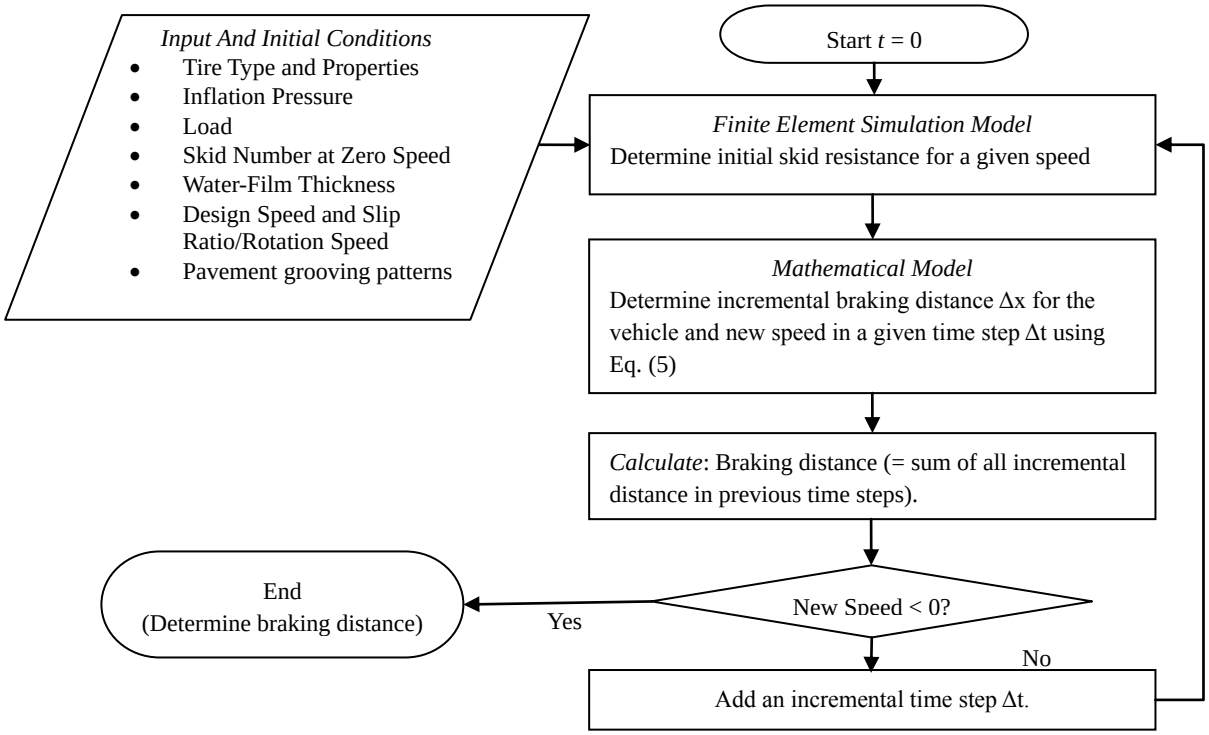

Fig. 3. Mechanistic Braking Distance Computation Framework (Adapted from [22]).

(t_w), wheel load (p), skid number at zero speed (SN_0), grooved width (w), grooved depth (d), groove center-to-center spacing (s) and groove pattern (Θ). Eqs. (5) and (6) are applied to estimate the braking distance for a vehicle and the corresponding computation procedure is illustrated in Fig. 3.

Analysis of Braking Distance Results

Using the computational procedure for braking distance described in Fig. 3, braking distance can be computed for different initial speeds. Table 5 lists the calculated braking distance for each pavement surface under different initial speed and water film thicknesses. It can be observed that braking distance on wet pavements increases with increasing water-film thickness. This is due to the fact that wet pavement skid resistance decreases with thicker water-film thickness. The highest rate of increase in braking distance for locked wheel on smooth pavement occurs when the water-film thickness reaches 4 mm. While for the case of ABS controlled wheel on grooved pavement, the rate of increase in braking distance tends to stabilize. Fig. 4 illustrates the effect of water-film thickness on braking distances (for a given initial speed of 80 km/h).

Table 6 further quantifies the percentage improvement in braking distance due to the application of ABS and the application of pavement grooving. It is clear from the table that in the presence of ABS control and pavement grooving, braking distance is significantly improved by 71.8% when compared to a locked wheel sliding on smooth pavement. The larger percent improvements at higher speeds indicate the effectiveness of these applications at high vehicle speeds. Moreover, it can be observed that the application of ABS control is more efficient than the application of pavement grooving under the same condition when the water-film thickness is less than 4 mm. For water thickness thicker than 4 mm, pavement grooving becomes more efficient at initial vehicle speeds higher than 60 km/h. This suggests the importance of providing escape channels when the water thickness is thick.

Table 6 also shows that when transverse grooves and ABS control are both applied, the combined improvements are higher than when the two measures are applied singly. The percent improvement of braking distance by combining the two applications becomes more significant with increasing water thickness and initial speed.

Conclusions and Future Work

This paper has presented a 3-dimensional finite element simulation model to evaluate the improvement of pavement frictional performance of transversely grooved pavement surfaces under different driving conditions. The simulation model was applied to determinate the skid resistance and braking distances of vehicles moving on smooth pavement and transversely grooved pavements respectively. The skid resistance simulation model is capable to simulate vehicle slip on wet pavements and is validated against past experimental results. It is found from the analyses presented in the paper that skid resistance is higher for wheels equipped with ABS as opposed to locked wheels. Using the mechanistic braking distance computation framework presented in the paper, It is found that use of pavement grooving and ABS is more apt in providing safe braking as compared to the condition of locked wheel on smooth pavements. This paper considers tire longitudinal slip only. Future studies will improve the proposed simulation model by taking into account lateral slip angle.

References

Table 5. Braking Distances for Different Initial Speeds and Water-film Thicknesses.

Water-film Thickness [mm]	Initial Vehicle Speed [km/h]	Predicted Braking Distance for Locked Wheel [m]		Predicted Braking Distance for ABS Controlled Wheel [m]	
		Smooth Pavement	Grooved Pavement	Smooth Pavement	Grooved Pavement
0.5	20	2.7	2.4	2.0	1.9
0.5	40	10.6	9.5	7.4	6.8
0.5	60	27.8	22.3	18	15.6
0.5	80	58.3	40.9	35	28.2
0.5	100	102.5	67.4	62.9	45.5
1.0	20	2.8	2.5	2.2	2.0
1.0	40	10.9	9.7	7.5	6.9
1.0	60	29	22.5	18.1	15.8
1.0	80	62.6	41.4	35.2	28.7
1.0	100	113.6	68.1	64.3	46.5
3.8	20	2.9	2.6	2.4	2.1
3.8	40	11.5	9.9	8.5	7.0
3.8	60	33	22.7	22.4	16.0
3.8	80	76.3	42.1	46.3	29.3
3.8	100	156.6	69.0	84.6	48.1
7.5	20	3.1	2.8	2.7	2.2
7.5	40	12.3	10.2	8.8	7.1
7.5	60	37.1	23.0	25.3	16.6
7.5	80	91.5	43.6	58.9	30.9
7.5	100	181.3	75.6	96	51.2

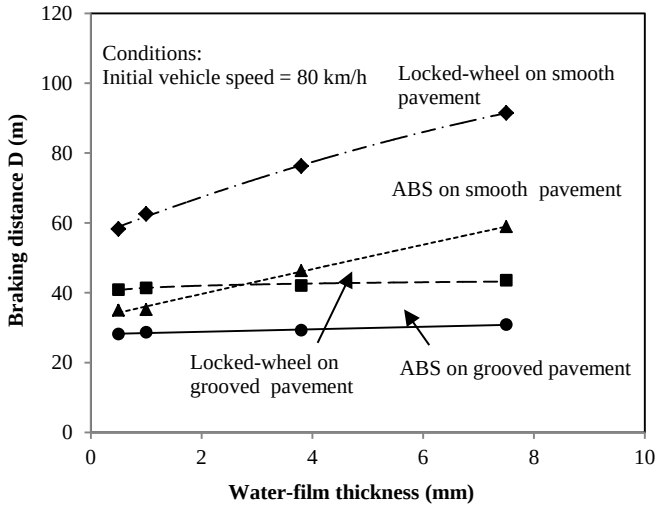

Fig. 4. Effect of Water Film Thickness on Braking Distances.

1. Zuieback, J.M. (1977). Methodology for establishing frictional requirements, *Transportation Research Record*, No. 623, pp. 51-61.
2. Cairney, P. and Germanchev, A. (2006). A pilot study of the effects of macrotexture on stopping distance, *Road Safety Research and Analysis Report*, CR 226. Australian Road Research Board, Canberra, Australia.
3. Hall, J.W. Smith, K.L. and Littleton, P. (2009). Texturing of concrete pavements, *NCHRP Report 634*, National Research Council, Washington, DC, USA..
4. Sugg, R.W. (1969). Joint NASA-British Ministry of Technology skid correlation study: results from British vehicles, *Pavement Grooving and Traction Studies*, NASA SP-5073, pp. 361-410, National Aeronautics and Space

Table 6. Percentage Improvement in Braking Distance Due to Groove and ABS Application.

Water-film Thickness [mm]	Initial Vehicle Speed [km/h]	Percentage Improvement in Braking Distance Due to		
		Groove Application for Locked Wheel Case	ABS Application for Smooth Pavement	Groove and ABS Application
0.5	20	7.7%	23.1%	26.9%
0.5	40	10.4%	30.2%	35.8%
0.5	60	19.8%	35.3%	43.9%
0.5	80	29.8%	40.0%	51.6%
0.5	100	34.2%	38.6%	55.6%
1.0	20	9.1%	20.0%	27.3%
1.0	40	11.0%	31.2%	36.7%
1.0	60	22.4%	37.6%	45.5%
1.0	80	33.9%	43.8%	54.2%
1.0	100	40.1%	43.4%	59.1%
3.8	20	10.3%	17.2%	27.6%
3.8	40	13.9%	26.1%	39.1%
3.8	60	31.2%	32.1%	51.5%
3.8	80	45.3%	39.3%	61.6%
3.8	100	55.9%	46.0%	69.3%
7.5	20	9.7%	12.9%	29.0%
7.5	40	17.1%	28.5%	42.3%
7.5	60	38.0%	31.8%	55.3%
7.5	80	52.3%	35.6%	66.2%
7.5	100	58.3%	47.0%	71.8%

Administration, Washington, DC, USA.
5. Horne, W.B. (1969). Results from studies of highway grooving and texturing at NASA Wallops station, Pavement grooving and traction studies. *NASA SP-5073*, pp. 425-464, National Aeronautics and Space Administration, Washington, DC, USA.
6. Clemett, H.R. and Moules, J.W. (1973). Brakes and skid resistance, *Highway Research Record*, No. 477, pp. 27-33.
7. MacAdam, C.C. and Fancher, P.S. (1978). Survey of antilock system properties, *UM-HSRI-78-47 Final Report*, Highway Safety Research Institute.
8. Sahin, M. and Unlusoy, Y.S. (2010). Design and simulation of an ABS for an integrated active safety system for road vehicles, *International Journal of Vehicle Design*, 52, pp. 64-81.
9. Sugai, M., Yamaguchi, H., Miyashita, M., Umeno, T., and Asano, K. (1999). New control technique for maximizing braking force on antilock braking system, Vehicle System Dynamics: *International Journal of Vehicle Mechanics and Mobility*, 32(4/5), pp. 299-312.
10. Cho, J.R., Lee, H.W., and Yoo, W.S. (2007). A wet-road braking distance estimate utilizing the hydroplaning analysis of patterned tire, *International Journal for Numerical Methods in Engineering*, 69, pp. 1423-1445.
11. Anwar, S. and Ashrafi, B. (2002). A predictive control algorithm for anti-lock braking system, *Society of Automotive Engineers Technical Paper*, 2002-01-0302.
12. Harifi, A., Aghagolzadeh, A., Alizadeh, G., and Sadeghi, M. (2008). Designing a sliding mode controller for slip control of antilock brake system, *Transportation Research Part C*, 16(6). pp. 731-741.
13. ADINA R&D Inc. (2010). ADINA 8.7 Theory and Modeling Guide Volume I: ADINA Solids and Structures, ADINA R&D Inc., Watertown, Massachusetts, USA.
14. ADINA R&D Inc. (2010). ADINA 8.7 Theory and Modelling Guide Volume III: ADINA CFD and FSI, ADINA R&D Inc., Watertown, Massachusetts, USA.
15. Ong, G.P. and Fwa, T.F. (2007). Prediction of Wet pavement skid resistance and hydroplaning potential, *Transportation Research Record*, No. 2005, pp.160-171.
16. Ong, G.P. and Fwa, T.F. (2007). Wet-pavement hydroplaning risk and skid resistance: modelling, *Journal of Transportation Engineering*, 133(10), pp. 590-598.
17. American Society for Testing and Materials, (2011). ASTM Standard E524-11. standard specification for standard smooth tire for pavement skid-resistance tests, *ASTM Standards Sources*, ASTM, Philadelphia, PA, USA.
18. American Society for Testing and Materials. (2011). ASTM Standard E274-11. Standard test method for skid resistance of paved surfaces using a full-scale tire, *ASTM Standards Sources*, ASTM, Philadelphia, PA, USA.
19. Horne, W.B. and Tanner, J.A. (1969). Joint NASA Ministry of Technology skid resistance correlation study results from American Vehicles, *Pavement Grooving and Traction Studies*, NASA SP-5073, pp. 325-359, National Aeronautics and Space Administration, Washington, DC, USA.
20. Sacia, S.R. (1976). The Effect of operating conditions on the skid performance of tires, *Transportation Research Record*, No. 621. pp. 126-135.
21. Gallaway, B.M., Ivey, D.L., Hayes, G.G., Ledbetter, W.G., Olson, R.M., Woods, D.L., and Schiller, R.E. (1979). Pavement and geometric design criteria for minimizing hydroplaning, Federal Highway Administration Report, *No. FHWA-RD-79-31*, Texas Transportation Institute, Texas A&M University.
22. Ong, G.P. and Fwa, T.F. (2010). Mechanistic interpretation of braking distance specifications and pavement friction requirements, *Transportation Research Record*, No. 2155, pp. 145-157.